(Preprint) AAS 23-305

TRAJECTORY DESIGN AND EARLY MISSION OPERATIONS FOR THE LUNAR ICECUBE MISSION

Robert E. Pritchett[*], David C. Folta[†], Sun Hur-Diaz[*], Kyle Hughes[*]

The Lunar IceCube (LIC) mission, a Next Space Technologies for Exploration Partnerships (NSTEP) program selection, was launched as a rideshare onboard Artemis-I on November 16^{th}, 2022, and deployed into a high energy lunar flyby trajectory. The final destination of the mission was a polar elliptical lunar orbit from which it could conduct spectroscopy observations of the lunar surface; however, a near rectilinear halo orbit (NRHO) was planned to be used as a staging orbit that divided the lunar transfer and low-thrust spiral phases of the mission. This paper presents the process used to design the LIC transfer trajectory from the high-energy deployment state to a 9:2 synodic resonance NRHO. Additional analyses performed, to assess the critical deployment to lunar flyby phase of the trajectory and to generate recovery trajectories following a loss of contact with the spacecraft, are described as well. Lessons learned from working on the LIC mission are presented to inform the design of similar future CubeSat missions.

INTRODUCTION

Lunar IceCube (LIC), a 6U CubeSat, was selected for participation in the Next Space Technologies for Exploration Partnerships (NSTEP) program, which leverages partnerships between public and private entities to develop the deep space exploration capabilities necessary for the next steps in human spaceflight. The LIC mission, led by the Space Science Center at Morehead State University (MSU), was supported by scientists and engineers from NASA Goddard Spaceflight Center (GSFC).[1,2] Specifically, GSFC provided the trajectory design, maneuver planning, navigation and tracking support, and attitude support. LIC and nine other CubeSats were included as secondary payloads on the maiden voyage of the Space Launch System (SLS), called Artemis-1. These CubeSats were deployed, four or more hours after launch, onto high-energy trajectories that resulted in a lunar flyby and, in many scenarios, eventual escape from the Earth-Moon system if no maneuvers were performed.

The science objectives of the LIC mission required the design of a trajectory to take the spacecraft from its high-energy escape trajectory at deployment to a low-lunar orbit. This challenging design problem was complicated by the limited control authority of the LIC spacecraft due to its very low-thrust propulsion system, and the need to adapt quickly to changes in launch epoch necessitated by the primary mission. The complexity of the LIC mission design problem garnered interest from many researchers who proposed innovative approaches for designing the LIC trajectory.[3–6] The work of these authors along with that of GSFC engineers resulted in the design process that was ultimately employed for the construction of a baseline LIC trajectory. This paper presents this

[*]Aerospace Engineer, NASA Goddard Space Flight Center, Greenbelt, MD, 20771, USA.
[†]Aerospace Engineer, AIAA Senior Fellow, NASA Goddard Space Flight Center, Greenbelt, MD, 20771, USA.

design process along with steps that were taken during the early stages of the LIC mission when a loss of contact with the spacecraft necessitated the rapid design of recovery trajectories that could deliver LIC to its science orbit. Special attention is also paid to the operational constraints that influenced trajectory design and analysis for the first few days following spacecraft deployment prior to the initial lunar flyby. While a loss of signal ultimately prevented the successful completion of the LIC mission, the methods presented in this paper offer a foundation that can be built upon by future secondary payloads on missions destined for the Moon. Similar opportunities are already planned, and more are sure to arise as public and private space organizations continue a planned return to the Moon.

BACKGROUND

Software Tools

Two different software tools were used to develop the baseline LIC trajectory: the Systems Tool Kit (STK) and the Evolutionary Mission Trajectory Generator (EMTG). STK is a widely used mission design tool that, among other features, enables the construction of complex differential corrections and optimization problems that can incorporate states defined in a variety of state representations and reference frames. This capability, along with the mission design team's familiarity with this tool, is why STK was used to generate the initial trajectory designs that were subsequently passed to the trajectory optimization tool, EMTG. Additionally, because STK was intended to be the primary tool for LIC operations, this software was also used to reconverge EMTG outputs in a high-fidelity dynamical model. When the final version of the LIC baseline trajectory was converged, STK was able to easily generate a number of products that were provided to other members of the LIC team in charge of navigation and operations.

EMTG solves optimization problems via an inner and an outer loop. The inner loop typically employs a forward/backward shooting framework to transcribe the optimization problem, and the resulting nonlinear programming problem (NLP) is solved using the Sparse Nonlinear OPTimizer (SNOPT).[7,8] The EMTG outer loop utilizes a monotonic basin hopping (MBH) strategy to perturb the initial guess supplied to each iteration of the inner loop to attempt to identify a global optimal solution. A variety of trajectory optimization problems have been successfully solved using EMTG;[9,10] however, this tool has typically been applied to chemical and low-thrust interplanetary transfers. Therefore, a modified EMTG design process was developed to accommodate the tool's application in the cislunar environment where the interaction of the Earth, Moon, and Sun results in a chaotic dynamical regime.

Dynamical Models

Several different dynamical models available within each trajectory design software were utilized to develop the LIC baseline trajectory. Using multiple dynamical models with different levels of fidelity enabled a more efficient design process than if a highly accurate but computationally burdensome model had been used for the entire process. Within EMTG, two dynamical models, a low-fidelity and a medium-fidelity model, were used. The first of these two models was a two-body dynamical model that included averaged N-body perturbations and used the Sims-Flanagan technique to approximate low-thrust maneuvers. The Sims-Flanagan transcription enables trajectory segments to be propagated analytically via Kepler's equations which significantly decreases the computational time required to find a solution. This dynamical model and its use in EMTG is described in greater detail by Englander, Folta, and Hur-Diaz.[11] The medium-fidelity model utilized

in EMTG is a point-mass ephemeris model that included the gravitational forces of the Earth, Moon, and Sun along with perturbing accelerations due to solar radiation pressure (SRP). Depending on the phase of the trajectory, either the Earth or the Moon was used as a central body. In this model an 8^{th} order Runge-Kutta integration algorithm was used to propagate spacecraft trajectories. The dynamical models available in EMTG enable rapid computation of an optimal trajectory and some refinement of this trajectory in a more accurate dynamical model; however, a different tool capable of greater accuracy is required to produce the final baseline trajectory.

STK was employed for the production of an initial design for the LIC baseline trajectory and for the generation of a final high-fidelity solution; in each case somewhat different dynamical models were used. When STK was used for initial trajectory design, the force model used a 4x4 or 8x8 EGM2008 Earth gravity model and included the Moon and Sun along with SRP as perturbing forces. The inclusion of both the gravitational and SRP forces caused by the Sun was essential because the accelerations imparted by these forces had a particularly large impact on the low-energy transfer trajectory used by LIC to reach its destination NRHO. When STK was used to converge a final high-fidelity version of the LIC baseline trajectory, more perturbing forces were included in the dynamical model. In this case, the force model included 30x30 EGM2008 Earth gravity, SRP, and third body forces from Moon, Sun, Mercury, Venus, Mars, Jupiter, Saturn, Uranus ,and Neptune. Finally, all of the different dynamical models used in EMTG and STK modeled the LIC low-thrust engine, a BIT-3 engine from Busek, as having constant thrust and constant specific impulse, I_{sp}. The maximum thrust magnitude, 1.1 mN, and I_{sp}, 2156 seconds, of this engine were based on testing and modeling of the BIT-3 conducted by Busek.[12]

BASELINE TRAJECTORY DEVELOPMENT

Development of the Lunar IceCube baseline trajectory was conducted in three stages: initial design generation, trajectory optimization, and high-fidelity refinement. Discontinuous initial estimates were created using designer expertise based on knowledge of dynamical systems theory applied within the circular restricted three-body problem (CRTBP). These initial estimates were supplied to EMTG which reduced trajectory discontinuities and enforced mission constraints to within a convergence tolerance and optimized the thrust profile to maximize the final mass of the spacecraft. In the final step of the design process, the optimized trajectory was reconverged in a high-fidelity dynamical model using Systems Tool Kit (STK), the tool that was used in operations to provide products for the control center and inputs for the navigation team.

The ultimate destination of the Lunar IceCube spacecraft was a polar elliptical science orbit with an equatorial periapsis altitude of 100 km; however, a near rectilinear halo orbit (NRHO), based on the orbit selected for the Gateway space station, was used as an intermediate destination. This decision simplified the design process by separating lunar capture and spiral down to the final science orbit into two relatively independent problems. The analysis presented in this paper focuses on trajectory design from deployment to the NRHO.

Initial Design Generation

The first step in the process of developing a baseline trajectory for the LIC mission was the creation of initial trajectory designs that provided preliminary estimates for the spacecraft's state and control values along its transfer trajectory. These initial designs were supplied to the subsequent trajectory optimization step as a starting point for obtaining a mass optimal result. Complete continuity in position and velocity was not required for an initial design to be passed to the next step,

as the optimization process was frequently able to eliminate discontinuities while also minimizing propellant consumption. Nonetheless, strategies were applied to reduce discontinuities in the initial design as much as possible. These techniques were based off a combination of designer experience and familiar trajectory corrections procedures.

Several missions that preceded LIC, and which operated in either the Earth-Moon or Sun-Earth multibody dynamical regimes, provided valuable experience that was applied to develop initial designs for LIC. Involvement with the cislunar mission Artemis/Themis was particularly relevant because this mission used multiple lunar flybys and dynamical systems techniques to place two spacecraft into Earth-Moon L1 and L2 libration point orbits. Furthermore, recent Sun-Earth missions like the Deep Space Climate Observatory (DSCOVR) provided additional experience designing transfer to libration point orbits. Moreover, GSFC engineers benefitted from collaborations with university researchers who developed innovative approaches for designing the LIC trajectory that leveraged the unique features of the restricted three-body problem and bicircular restricted four-body problem.[3–6] These simplified dynamical models were used to rapidly generate many trajectory segments that were propagated forward and backward in time, and then assembled into initial designs for the LIC trajectory using inventive mapping techniques to select trajectory segments with minimal discontinuities between them. The approaches developed by these researchers along with experience garnered from prior libration point orbit missions informed the final initial design generation procedure.

The procedure used to produce an initial design for the LIC baseline trajectory involved the generation of forward and backward propagated trajectory segments that were iteratively updated to reduce discontinuities in time, position, and velocity between the two segments. This iterative process included the use of differential corrections techniques along with successive variations made "by-hand" based on designer experience. The first step, was to calculate an initial deployment state for LIC using the state of the Interim Cryogenic Propulsion Stage (ICPS) at the expected deployment epoch. Greater detail on this step is provided in the section on deployment analysis. Once a deployment state was determined this state was propagated forward in time through the initial lunar flyby using the point mass ephemeris model described previously. The forward propagated trajectory included a 1.5 days thrust arc that occurred approximately 1.5 days after deployment, and the remainder of the trajectory was purely ballistic. The thrust arc utilized the max thrust of the LIC ion engine for the entirety of the maneuver. The B-plane state of the initial lunar flyby was iteratively adjusted by changing the direction of the thrust vector during the pre-flyby maneuver to produce a post-flyby LIC trajectory that returned to the Earth-Moon system.

After a forward propagated trajectory that returned to the Earth-Moon system following the initial lunar flyby was created, a differential corrections process was employed to further update the flyby B-plane state to produce a return trajectory with a geometry that was favorable for reaching the destination 9:2 NRHO. Intermediate targets in the Sun-Earth rotating frame provided the constraints of the differential corrections process while the variables were the components of the pre-flyby thrust vector. The targets were selected based on knowledge of the common geometries of ballistic lunar transfer (BLT) trajectories[13] within the different quadrants of the Sun-Earth rotating frame. This geometry involved one ore more apses beyond the radius of the Moon's orbit. If the targeting procedure failed to converge upon a solution, then post-flyby trajectory corrections maneuvers (TCMs) were added to provide the additional change in energy required to reach the target state. When TCMs were added, the differential corrections problem was reformulated, so that only the thrust vector of the most recent TCM was permitted to change to hit the desired target. Succes-

sive addition of intermediate targets and TCMs eventually produced a trajectory that returned to the Earth-Moon system with a geometry that was favorable for 9:2 NRHO insertion.

Next, a trajectory that was propagated backwards in time from the destination 9:2 NRHO was created. Ephemeris data for the 9:2 NRHO that will be employed by the Gateway was provided by NASA Johnson Space Center (JSC) engineers,[14,15] and this data spanned 2025 to 2025. A state at which to begin the backward propagation was selected from the 9:2 NRHO ephemeris data. This arrival state was chosen such that its epoch was approximately one year after LIC deployment and its location on the NRHO was near apolune. These criteria were based on prior experience designing low-energy transfers to the Moon and trajectories for NRHO insertion or departure. A trajectory that departed the NRHO at the selected ephemeris state, in reverse time, was created by applying a 7 day low-thrust maneuver that used the maximum LIC thrust magnitude of 1.1 mN. A trajectory was propagated backward in time ballistically at least until the epoch at the end of the forward propagated trajectory was reached. After the forward and backward propagated trajectory arcs were created, a refinement process was begun that gradually decreased the discontinuity between the two arcs.

Following the initial generation of the forward and backward propagated trajectory segments, large discontinuities in position, velocity, and mass typically existed at the epoch where these segments met. These discontinuities were reduced, if not eliminated, using a differential corrections process. The variables of this process were the components of the thrust vector for each of the maneuvers included in the forward propagated trajectory along with those of an additional capture maneuver that was added to the backward propagated trajectory. The constraints of the differential corrections process were continuity in position and epoch between the two trajectory segments. If this targeting problem was successfully converged, then the result was used in a subsequent targeting problem where velocity continuity was enforced. For some initial designs, complete continuity between the trajectory segments could be achieved; however, often at least some discontinuity still existed even if the magnitude of this discontinuity was reduced by the corrections process. An example of the discontinuity that often remained in an initial guess is shown Figure 1 where a velocity discontinuity between the forward and backward propagated segments is evidenced by the deviation between these two segments. A discontinuity in the mass of the forward and backward propagated segments often remained as well.

The results of the initial design stage of the baseline trajectory design process were passed to the subsequent trajectory optimization stage as a series of waypoints and durations. The number of waypoints that the initial design was discretized into changed with the launch date, but the number typically varied between 3 and 5. This information was used to replicate the geometry of the initial design while adding, removing, or modifying maneuvers as needed to remove discontinuities and achieve an optimal result. The trajectory shown in Figure 1 exhibits one of four different geometries that the LIC trajectory assumed, depending on the launch epoch. However, the initial design generation process remained the same regardless of the geometry of the transfer. The primary difference in geometries was the number of TCMs that were required and the duration of the NRHO capture maneuver. Some geometries tended to be more challenging to create an initial design for, and these designs possessed larger discontinuities when they were passed to the trajectory optimization step.

Trajectory Optimization

Initial designs formulated in the first stage of the design process were supplied to EMTG which enforced mission constraints and minimized the propellant mass required to reach the destination

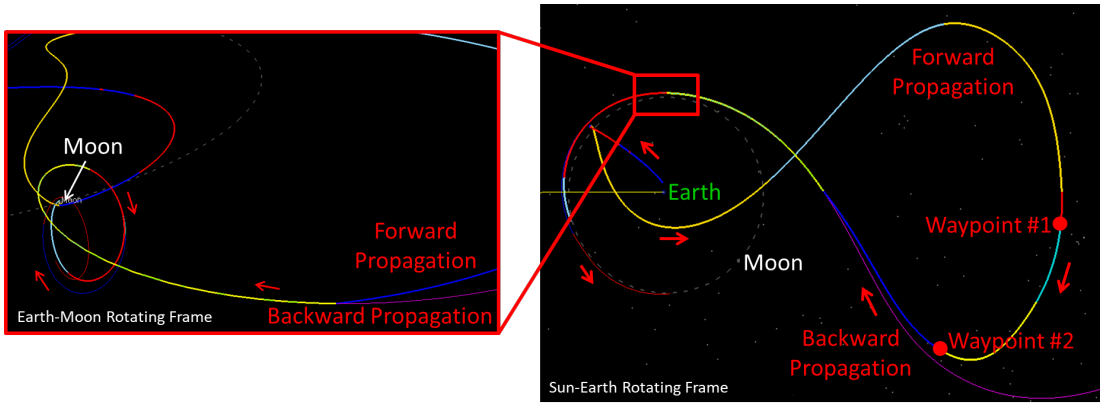

Figure 1: Forward and backward propagated trajectory segments generated during the initial design process for the LIC baseline transfer trajectories. The velocity discontinuity between the two segments is shown in the Sun-Earth rotating frame (right) and a zoomed in view presented in the Earth-Moon rotating frame is also provided (left).

NRHO. The use of EMTG was essential for transforming initial designs for the Lunar IceCube baseline trajectory into optimized trajectories that could be easily reproduced in the final high-fidelity refinement step. EMTG was applied in an iterative process that incrementally increased the fidelity of the dynamical model and included additional constraints that were necessary to ensure a solution that was suitable for spacecraft operations.

In the first step of the optimization process, the initial design generated in the previous stage was constructed one waypoint at a time using the medium-fidelity model described previously that employs the Sims-Flanagan transcription to model low-thrust maneuvers and third-body perturbations. In general, the trajectory spanning two waypoints of the initial design was represented as a single phase in the optimization problem first constructed for EMTG. The exception to this rule was the pre-flyby portion of the LIC trajectory where more phases were used to model distinct portions of LIC's early mission operations. A diagram that illustrates the structure of the optimization problem set up in EMTG is shown in Figure 2. An important feature of the optimization problem setup was that the central body that states along the trajectory were defined with respect to was changed from the Earth to the Moon when the trajectory entered the sphere of influence (SOI) of the Moon. Switching between central bodies resulted in a more numerically well-conditioned optimization problem. Additionally, unless indicated otherwise in Figure 2, the thrust magnitude used by LIC in the phases following the initial lunar flyby was permitted to vary between zero and the maximum thrust level. An example of the thrust profile that results from permitting this freedom is displayed in Figure 3a. While this type of thrust profile is not physically realizable, allowing flexibility for the thrust magnitude and phase duration aids the optimizer in identifying an optimal solution. The thrust profile is updated in subsequent steps to ensure compliance with operational constraints. The flexibility allowed in the optimization problem and the speed of the Sims-Flanagan transcription proved essential because multiple "hops" of the MBH outer loop were often required to identify a solution that resolved discontinuities in the initial design provided to EMTG.

Another key decision that facilitated the computation of an optimal solution was constraining the final state of the LIC transfer in the Earth-Moon rotating frame and permitting the arrival epoch to vary over the span of two months. Initially, a transfer trajectory was converged that matched the

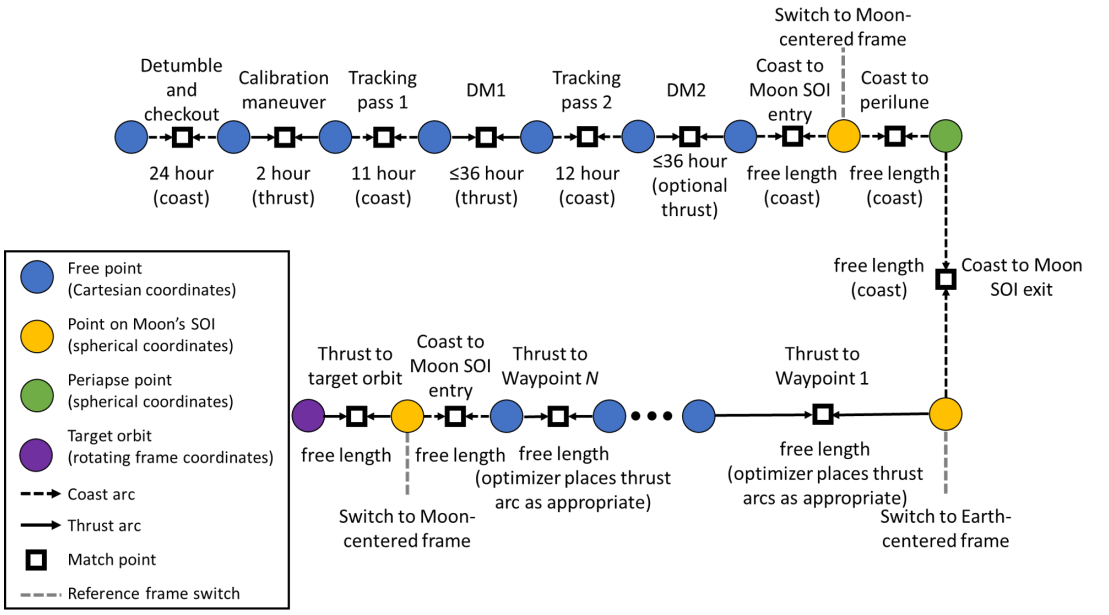

Figure 2: Journey structure employed for EMTG optimization problem; derived from a figure created by Englander, Folta, and Hur-Diaz.[11]

exact inertial frame state and epoch on the NRHO that was delivered with the initial design. After a solution was obtained, the final state constraint was changed to a rotating frame constraint, and the values for this constraint were calculated by transforming the final inertial state in the initial design to the Earth-Moon rotating frame at the final epoch. However, the final epoch of the transfer was allowed to vary by up to a month before or after the original final epoch. The variation in epoch meant that the final inertial state of the LIC transfer would change, but because the rotating frame state remained constant, the spacecraft was guaranteed to enter an "NRHO-like" orbit at the end of the transfer. This orbit could then be corrected to provide the phasing and longevity required by subsequent stages of the LIC mission.

Next, the solution converged using the medium-fidelity dynamical model was reconverged in the more accurate point-mass ephemeris dynamical model described previously in which trajectory

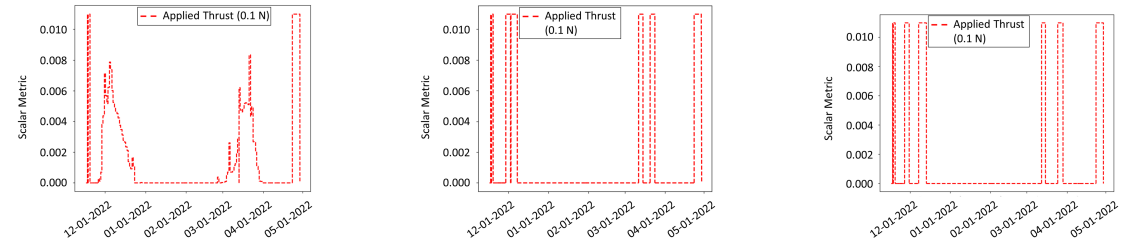

(a) Initial Result (b) Discrete Thrust and Coast (c) With Navigation Coasts

Figure 3: Thrust profile refinement process for the LIC transfer trajectory generated with EMTG for a launch date of November 16, 2022.

segments are explicitly propagated. The resulting trajectory is much more accurate because perturbations from the low-thrust engine and third-bodies are included at each integration time step. Typically, the LIC baseline could be reconverged in the higher fidelity transcription with a single solve of the NLP. The ease of this transition demonstrates that the Sims-Flanagan transcription can be effectively applied even in multi-body dynamical regimes. The conversion process only encountered difficulty if an insufficient number of time steps was used to discretize the lower-fidelity trajectory, particularly for the dynamically sensitive initial lunar flyby and final lunar approach. The number of time steps used in the lower-fidelity trajectory dictates the number of points at which perturbations are included to model the impact of low-thrust maneuvers and third-body accelerations. If the number of time steps for a given phase of the optimization problem is set too low, then the changing dynamics during that phase will not be adequately captured leading to difficulty reconverging the solution in a higher-fidelity model where a more complete representation of dynamical trends is simulated. If challenges were encountered when transitioning the low-fidelity solution to the higher-fidelity model, then the lower-fidelity solution was reconverged with a greater number of time steps.

Finally, the higher-fidelity trajectory was refined by first subdividing all phases into distinct thrust and coast arcs and then restricting the duration and frequency of thrust arcs. A new optimization problem setup was created by subdividing phases that included thrusting and coasting into multiple smaller phases in which the spacecraft was required to exclusively thrust or coast. Moreover, thrusting phases were required to use the maximum available thrust magnitude for the duration of the phase. The new phase structure of the optimization problem was determined by assessing the initial thrust profile, displayed in Figure 3a, and defining the start of a thrust phase at the time when the thrust magnitude rises above a threshold value, typically half of the maximum thrust magnitude. The end of a thrust phase and the start of a subsequent coast phase was defined at the time that the thrust magnitude dropped back below the threshold value. Once the new structure for the optimization problem was defined the problem was reconverged, and an example of the resulting thrust profile is shown in Figure 3b. The LIC baseline trajectory was subdivided into discrete thrust and coast arcs because the BIT-3 low-thrust engine operates at discrete thrust magnitudes and are not able to throttle to all magnitudes between zero and their maximum capability. Moreover, the optimal thrust profile for a low-thrust transfer typically exhibits a "bang-bang" profile where the thrust magnitude either equals its maximum available value or is at zero. Thus, by forcing the thrust profile of the LIC trajectory to abide by this known behavior, an optimal solution is more easily assured.

The practical limitations of the LIC spacecraft necessitated that all thrust maneuvers last no more than 7 days, and that at least seven days of coasting follow each thrust arc to allow time to perform navigation activities before thrusting resumes. Scripts were written to discretize each high-fidelity solution such that navigation coast arcs were inserted and thrust arcs that exceeded the maximum duration were broken up. The discretization process introduced constraint violations in the high-fidelity solution, therefore, the trajectory was reconverged to produce a continuous transfer trajectory that satisfied all problem constraints including the newly added navigation coast periods and maximum thrust arc durations. The plot displayed in Figure 3c is one example of what the LIC thrust profiles looked like following completion of this final refinement step. After the new high-fidelity EMTG solution was computed, the resulting trajectory was exported as a .bsp file along with several text files that summarized key maneuver and target information. An example of the final optimized version of the LIC trajectory computed with EMTG is displayed in Figure 4. A

.bsp file of this solution along with several text files containing data on the timing and direction of low-thrust maneuvers were generated for use in the final high-fidelity refinement step.

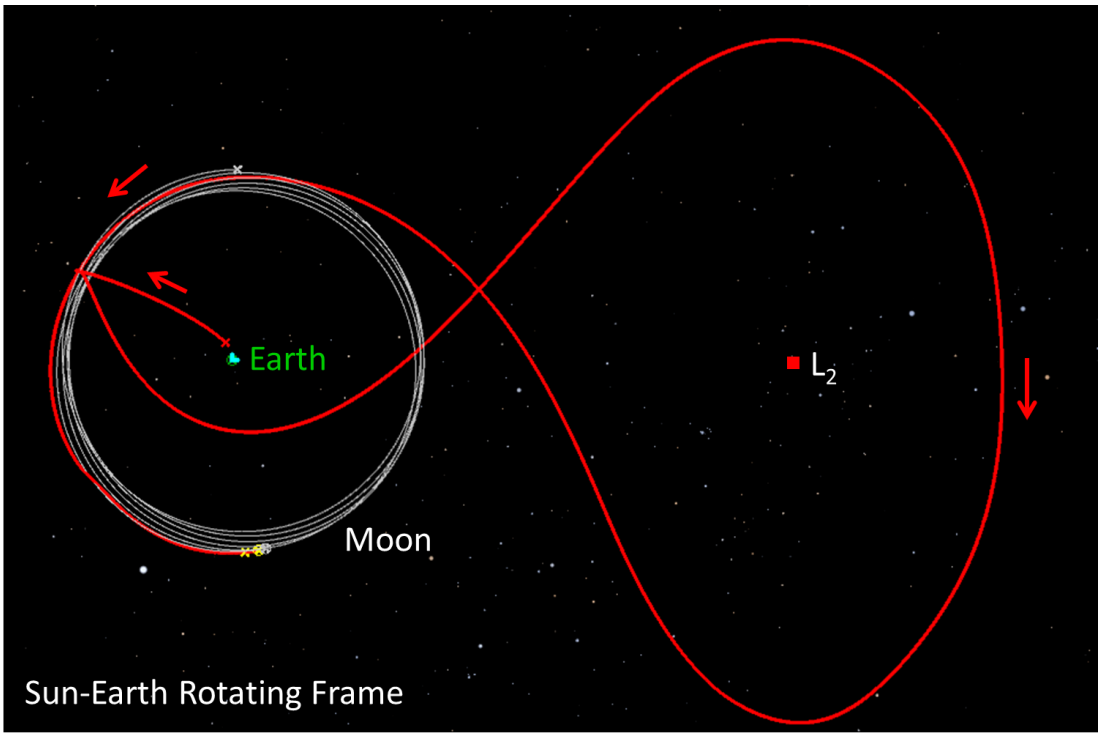

Figure 4: Optimized LIC transfer trajectory computed with EMTG.

High-Fidelity Refinement

The tool baselined for operations, STK/Astrogator, was used to finalize the trajectory design. The SNOPT module was used to sequentially perform forward shooting to match the states at the end of each thrust arc from the EMTG solution. A MATLAB script was developed to automatically parse the maneuver and target output files that EMTG generates, create target sequences in the Astrogator mission sequence, and execute each target sequence until convergence. The MATLAB script executed each target sequence sequentially until all the coast and maneuver segments from the EMTG solution had been modeled. This forward propagated rendering of the EMTG solution in the high-fidelity operational STK/Astrogator tool ensured that the resulting trajectory would be more operationally achievable than the forward-backward transcription of EMTG. Each target sequence consisted of a coast arc followed by the individual maneuver segments associated with a continuous thrust arc. Typically, there were four maneuver segments in one thrust arc as modeled in EMTG. This provided enough control parameters in SNOPT to satisfy the target constraint. The target is the position and velocity states at the end epoch of the last maneuver segment from EMTG, and the variables consisted of the coast duration, the direction and duration of each maneuver segment, except the last one where only the direction is allowed to vary. For SNOPT to converge, the target constraints and the variables had to be properly scaled. Also, the constraint matching tolerance in the EMTG forward-backward solution had to be set sufficiently small for convergence in STK. The finalized trajectory designs for several potential trajectories within the final launch period considered by LIC are shown in Figure 5, and the propellant consumption and time of flight associated with

each of these results are presented in Table 1.

Once all the Coast-Thrust target sequences from EMTG were converged, the MATLAB script automatically generates several products for delivery including tracking schedule requirements based on the maneuvers, maneuver summary, and several ephemeris files (e.g., 28 days with no maneuver, 28 days after the next maneuver, and a long-term with all maneuvers), Astrogator Summary, thrust history file (for modeling nominal maneuvers in Orbit Determination Toolkit (ODTK)). Recipients of these deliverables include JPL's Deep Space Network (DSN), MSU's Mission Operations Center (MOC), and GSFC's Flight Dynamics Facility (FDF). The same process of setting up the STK/Astrogator target sequences is used in operations, ensuring that the nuances for a given trajectory is well understood.

The MATLAB script was automated as much as possible. Just a few input parameters, such as the directory name where the EMTG output files were located, needed to be updated to generate the final, high-fidelity solution. This automation eliminated potential human error in transposing data from EMTG to STK. It also significantly saved time as the launch period slipped regularly and high-fidelity trajectory data had to be delivered to the DSN on short notice.

Launch Date	Propellant Usage [kg]	Time of Flight [days]
11/14/22	0.084	166
11/15/22	0.093	165
11/16/22	0.120	163
11/17/22	0.142	162
11/18/22	0.143	188
11/19/22	0.047	187

Table 1: Propellant usage and time of flight for LIC baseline trajectory designs created for six possible launch days within launch period 28 (LP28) of the Artemis-1 mission

EARLY MISSION OPERATIONS

The roughly five days between spacecraft deployment and the initial lunar flyby were one of the most critical phases of the LIC mission. Within this period, LIC had to complete checkout procedures, thruster calibration, and a crucial maneuver that targeted the B-plane state necessary for achieving the desired post-flyby trajectory. The tight timing of this mission phase required thorough analysis to be conducted ahead of time to ensure that mission operators could rapidly respond to any anomalies that occurred during this period.

Early Mission Concept of Operations

LIC activity prior to the initial lunar flyby followed a predetermined operations schedule. The exact schedule changed slightly with each launch date and according to the contact schedule provided by the DSN; an example operations schedule for an October 9^{th}, 2018 launch date is shown in Figure 6. LIC was deployed approximately 4 hours after the launch of the SLS. The first 24 hours following deployment was dedicated to spacecraft acquisition, detumble, and checkout. Following this, a one hour calibration burn would be performed. This burn provided thruster performance parameters that would be used to design the subsequent maneuver which targeted the lunar B-plane state of the initial lunar flyby. The maneuver for targeting the B-plane state was called, deterministic maneuver one (DM1), and was expected to begin approximately 1.5 days after deployment and last

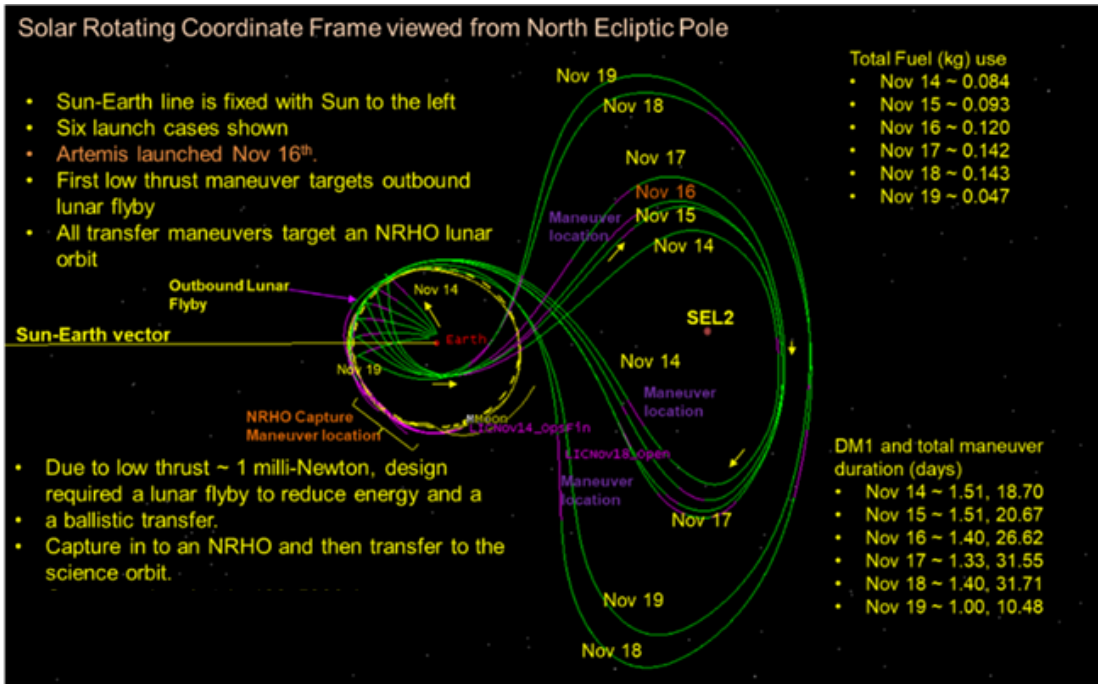

Figure 5: Lunar IceCube transfer trajectories, plotted in the Sun-Earth rotating frame and viewed from the North ecliptic pole, for launch dates from November 14 to 19, 2022.

no more than 1.5 days. Two additional opportunities for maneuvers prior to the lunar flyby were reserved in case DM1 did not result in a trajectory that met the targeted B-plane state; however, these maneuvers would only be performed if they were deemed necessary. The first of these backup maneuvers was denoted DM2 and would begin 3.5 days after deployment, while the final maneuver opportunity was called a trajectory correction maneuver (TCM) and was scheduled for 4.75 days after deployment. If necessary, the duration of the TCM was expected to be brief because perilune of the lunar flyby would be reached 5.25 days after deployment.

The lunar flyby shortly after launch and the necessity of performing a maneuver to target the correct flyby conditions were the primary drivers of the tight operations schedule for the early phase of the LIC mission. An additional complicating factor was the fact that the LIC team had limited control over the provided DSN contact times due to the many demands on the DSN, made by the Orion spacecraft and other rideshare CubeSats, during the early days of the Artemis 1 mission. While efforts were made by DSN personnel to match the contact schedule requested by the LIC team, deviations from this request occurred which further reduced the time available to the LIC flight operations team to perform orbit determination (OD) and replan maneuvers. To enable the LIC team to meet its tight schedule and respond rapidly to last minute changes, extensive analysis was performed to understand the impact of the LIC deployment conditions on the maneuvers LIC was expected to perform prior to the lunar flyby.

Deployment Analysis

The nine secondary payloads of the Artemis-1 mission were mounted within the Interim Cryogenic Propulsion Stage (ICPS), which separated from the Orion spacecraft about four hours after launch following the translunar injection burn. The expected ICPS state, orientation of its spin axis

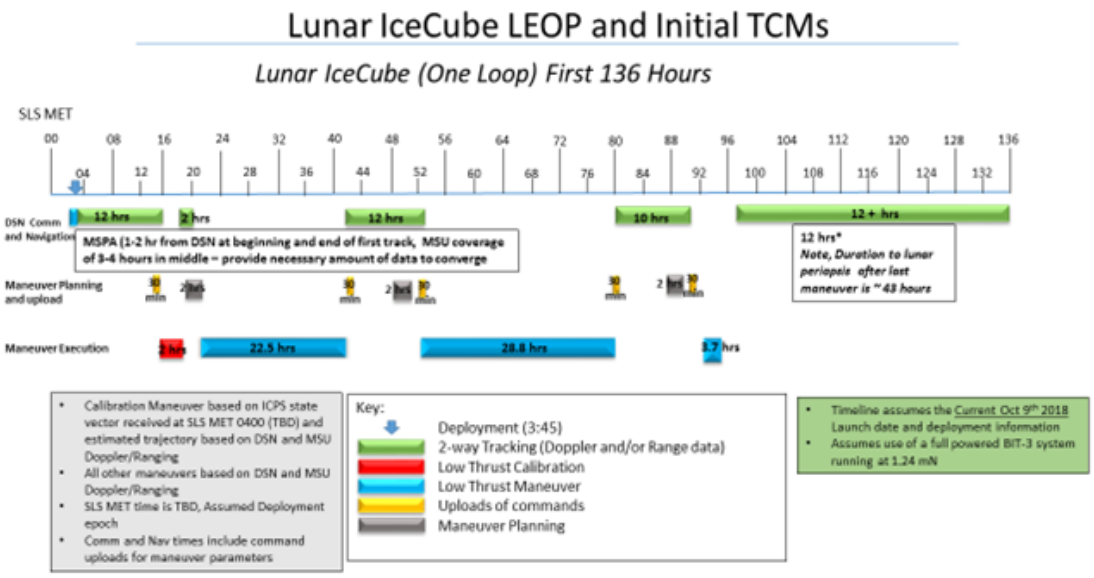

Figure 6: Example operations schedule for 10/9/18 launch date. From Morehead State University Final Report.[16]

with respect to the Sun line, and its spin rate at the deployment epoch was provided by the SLS team prior to launch. From this information, potential LIC deployment states could be computed. Figure 7 illustrates that the range of potential deployment states lay upon a cone whose angle was determined by the mounting of the CubeSat deployment mechanism relative to the spin axis of the ICPS. The baseline LIC trajectory was designed using a deployment state parallel to the spin axis

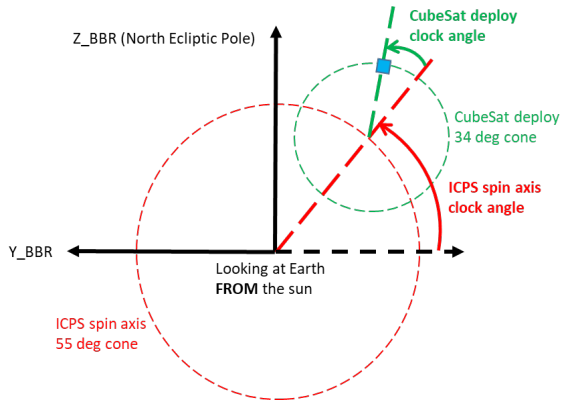

Figure 7: Sketch of the ICPS spin axis and CubeSat deployment clock angle relative to the ecliptic plane.

of the ICPS; however, in reality, the spinning ICPS would deploy LIC at a clock angle around the green cone shown in Figure 7. The seemingly minor variations in deployment state caused by the rotation of the ICPS about its spin axis, and the separation spring delta-v on the order of 1 m/s, led to significant differences in the B-plane states of the initial lunar flyby if no pre-flyby maneuvers were

performed, as highlighted in Figure 8. In this set of plots, created for a November 16th, 2022 launch

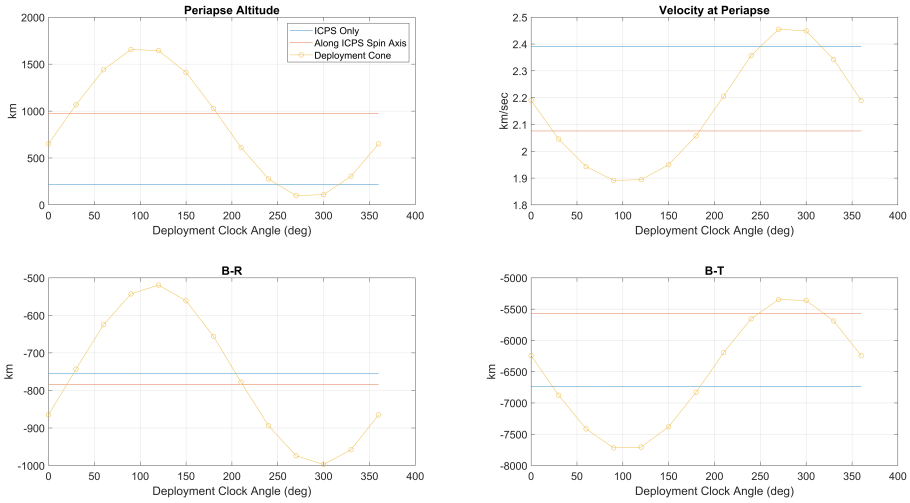

Figure 8: Changes in lunar flyby conditions as a function of deployment clock angle from the ICPS if no maneuvers are performed prior to the lunar flyby. Generated for the November 16th 2022 launch date.

date, the expected flyby altitude varies by 1500 kilometers depending on the clock angle. Therefore, the trajectory design and the early mission concept of operations (ConOps) had to consider the variation in the deployment clock angle about the ICPS spin axis. Notably, for some of the launch dates, there were deployment clock angles that would have led to lunar impact if no maneuver was executed. Using EMTG, trajectories corresponding to a range of potential deployment clock angles were computed and examined to answer two key questions regarding LIC early mission operations.

The first question to be answered was whether DM1 alone could be used to target the desired B-plane state, regardless of the deployment clock angle. The required analysis was accomplished using the Python EMTG Automated Trade Study Application (PEATSA)[17] which ran multiple EMTG optimization problems in parallel, each of which used different deployment conditions. Clock angles every 30° starting at 0° were used to generate 12 sets of deployment states, and these states were the starting point for 12 EMTG optimization problems. Aside from the difference in starting point, each optimization problem was identical and sought to reconverge the entire LIC trajectory from deployment to NRHO insertion. For the November 16th, 2022 launch date, each of the 12 optimization problems converged upon an optimal result, and Figure 9 displays how the duration of DM1 changed as a function of the deployment clock angle. Deployment clock angles of 120° and 150° required DM1 maneuvers that lasted the full 1.5 days allocated for this maneuver, while a DM1 of less than 0.5 days was needed for deployment clock angles of 300° and 330°. This full day variation in the required duration of DM1 demonstrates the importance of accounting for the deployment clock angle in the planning of the pre-flyby phase of the LIC trajectory. The cyan dotted line in Figure 9 denotes the DM1 duration that was computed when the ICPS spin axis was used to provide the initial LIC state rather than accounting for the variations due to clock angle. As expected, this approach to defining the LIC deployment state results in a DM1 duration that is approximately the average of the various durations that result when the clock angle is included. This result validates

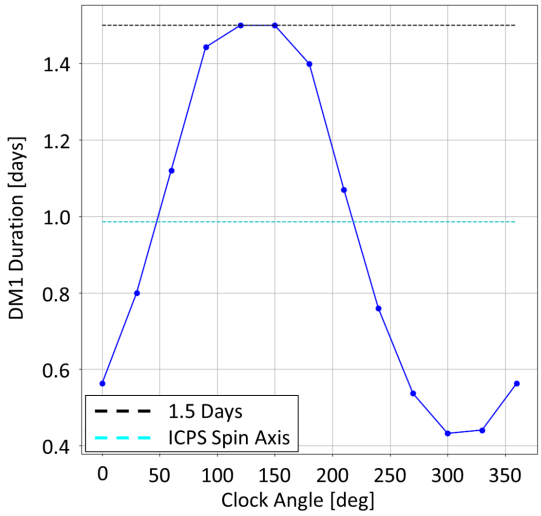

Figure 9: Change in DM1 duration as a function of deployment clock angle from the ICPS. Generated for a November 16th, 2022 launch.

the technique of using the ICPS spin axis as the initial state for the design of the LIC baseline trajectory. Finally, there were very few launch date and clock angle combinations analyzed where a 1.5 day DM1 was not sufficient to target the desired B-plane state; however, for the rare scenarios where this was the case DM2 could be added to complete the targeting problem.

The second question to be answered regarding LIC early mission operations was motivated by the brief window available in the timeline for the redesign of DM1 following LIC deployment. An analysis was conducted to determine whether "canned", that is, precomputed, calibration and DM1 maneuvers could be employed. Using canned maneuvers would simplify early mission operations either by eliminating the need to recompute the calibration and DM1 maneuvers, or, by at least, offering a backup option in the event that a new maneuver could not be calculated in time. PEATSA was again used to perform the required analysis by running 12 different EMTG optimization problems with unique deployment states in parallel. The canned maneuvers for each case were thrust directions for the calibration and DM1 maneuvers that were computed for an LIC baseline trajectory that used a state parallel to the ICPS spin axis to define the deployment state. Two sets of 12 EMTG runs were started, one which allowed a DM2 maneuver of up to 1.5 days and which started 0.5 days after the end of the 1.5 day period allocated to DM1. The other set of EMTG runs did not allow a DM2 maneuver. The set of EMTG runs that permitted a DM2 all converged upon an optimal solution and required a DM2 maneuver of 0.5 to 1 days to target the desired flyby conditions depending on the clock angle. Alternately, the set of EMTG runs that used a canned calibration maneuver and DM1 without a DM2 struggled to converge unless significant changes to the post-flyby thrust profile were permitted. The engineering effort required to incorporate these changes was deemed undesirable unless absolutely necessary, therefore it was decided that if a canned DM1 was used then DM2 would be executed to account for any differences between the expected and desired B-plane states as a result of the deployment clock angle. Together, the various analyses performed using EMTG offered confidence that a range of deployment scenarios and changes to the mission operations timeline could be accommodated while still achieving mission success.

RECOVERY ANALYSIS

A communications link with LIC was never established despite repeated attempts in the months following launch. In the initial days after deployment, it became clear that even if communication with LIC was established, there would be little to no time to perform the planned pre-flyby maneuver. Thus, efforts began to identify new trajectories that could transfer LIC to the desired NRHO despite the lack of a pre-flyby maneuver. Data from the SLS and several operational CubeSats deployed alongside LIC, was used to estimate a range of potential LIC trajectories. These trajectory estimates were then employed as a starting point for EMTG which was used to conduct a broad search for potential recovery trajectories. This analysis successfully identified several recovery trajectories that could be used to deliver LIC to its destination NRHO. The propellant usage to recover each trajectory is shown in Figure 10 over a span of anticipated (at the time) recovery dates. The color indicates the flight time, which generally decreases for later recovery dates/times. The suspected cause of this trend is a preferred Earth-Moon-Sun geometry, as all propellant-optimal solutions tend to insert into the NRHO on similar dates, around February 22, 2024 on average.

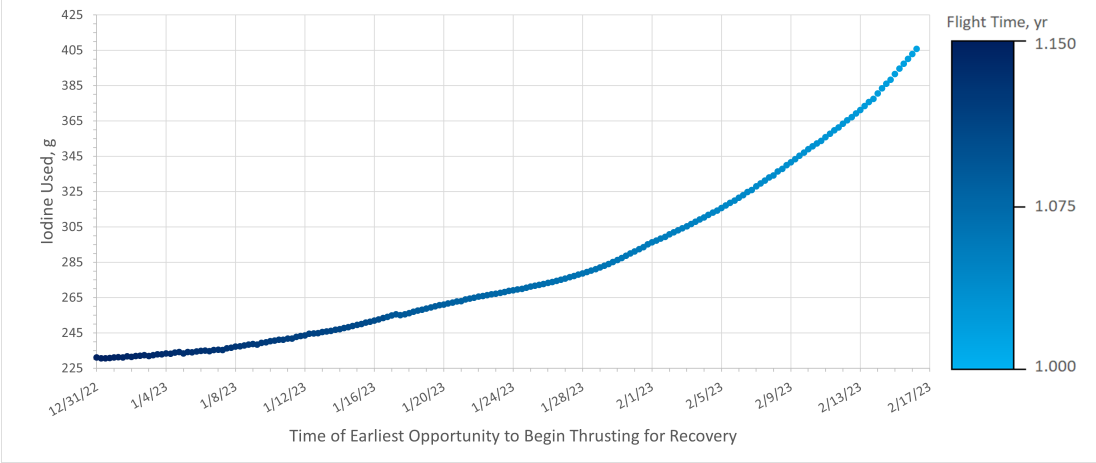

Figure 10: Electric propellant used to recover LIC starting from a variety of anticipated recovery dates and times. The recovery trajectories end after insertion into an NRHO. The color indicates the flight time, which ranges from 1 to 1.15 years.

LESSONS LEARNED

The LIC mission provided many valuable lessons that can inform the design of similar future CubeSat missions. Documenting and acting upon these lessons learned can reduce risk and increase the chances of success for future missions. Lessons learned from the LIC mission can be grouped into three main categories. Two of these categories are the impacts that the attitude control system (ACS) and power hardware had on the mission design and navigation of the LIC spacecraft. The final category deals with the consequences to LIC mission design of being a rideshare onboard the Artemis 1 mission. Many of these lessons learned are related to mission design and navigation, though the impact on this sub-discipline is sometimes indirect. The capabilities and requirements of the ACS had significant impacts on mission design and navigation for LIC that produced several valuable lessons. The first of these lessons is that thruster pointing constraints should be included early in the trajectory design process to avoid the need for time consuming revisions to the baseline trajectory. Power and thermal constraints resulted in several spacecraft attitudes that had to be

avoided. However, violation of these attitude "keep out zones" was not checked until after a baseline trajectory was computed, at which point, if an attitude violation was identified the trajectory would be updated to resolve the issue. The update process was iterative and required a high level of user involvement because no explicit way of enforcing the keep out zone constraints was available in the software used to compute the trajectory. Updating the trajectory design software to provide the ability to enforce pointing constraints and incorporating these constraints into the baseline trajectory design process would have saved a significant amount of time and been particularly helpful for redesigning maneuvers during time critical operations once LIC was in-flight.

An additional ACS lesson learned was that the frequency and duration of momentum wheel desaturation maneuvers should be considered earlier in the trajectory design process. The size of the momentum wheels used by LIC and the long duration of the maneuvers required by the low-thrust system meant that frequent momentum unloads would be necessary, and these could sometimes interrupt planned maneuvers. Moreover, the single gimbaled thruster of the low-thrust system was intended to be used for momentum desaturation maneuvers through the use of a closed loop control algorithm for determining the necessary spacecraft attitude and gimbal angle at each instant in time as the spacecraft center of mass changed. The frequency and the timing of these momentum unloads would have had significant impacts on the ability to accurately fly the LIC baseline trajectory because some maneuvers would be perturbed by momentum unloads that resulted in deviations from the baseline trajectory. Incorporating pointing constraints and the expected cadence and impact of momentum unloads earlier in the trajectory design process would have produced a baseline trajectory that required less frequent adjustments.

An additional lesson learned is related to the inability to track LIC during the many extended low-thrust maneuvers that were required to reach the destination orbit. The power limitations of the LIC spacecraft meant that it was not possible to communicate with Earth and operate the thruster simultaneously. This meant that maneuvers were to be performed "in the blind" and that the impact of these maneuvers would be determined in a subsequent orbit determination step. The absence of tracking and telemetry during maneuvers meant that if pointing or thruster performance errors resulted in a significant deviation from the planned trajectory, or if a spacecraft anomaly caused the early termination of a maneuver, these divergences would not be noticed and corrected until the conclusion of the scheduled maneuver. To mitigate the consequences of these occurrences, maneuvers were limited to no more than seven days and could not be followed by a maneuver for a period of one week, to provide sufficient time for orbit determination. However, even with this rule in place, the lack of tracking during maneuvers likely would have led to increased propellant consumption and delays in acquiring the spacecraft's signal following maneuvers. Another potential mitigation step would have been the inclusion of an accelerometer on the LIC spacecraft. Accelerometer data could be recorded during a maneuver and downlinked when communication was restored at the end of the maneuver. This data would have enabled maneuvers to be more accurately and more quickly reconstructed thereby facilitating the process of designing new maneuvers to account for any errors in maneuver execution. The accelerometer would have also allowed the implementation of a closed-loop onboard logic to control the burn duration based on the integrated delta-V. Unfortunately, an accelerometer was not in the design of the LIC spacecraft. In summary, for spacecraft utilizing low-thrust propulsion, which requires long duration maneuvers, it is critical to provide some tracking capability during these maneuvers to be able to quickly respond to anomalies.

Another set of lessons learned stems from the fact that LIC was a rideshare on the Artemis 1 mission. This situation was somewhat unique because the launch vehicle for this mission, the

Space Launch System (SLS), was conducting its maiden voyage after a lengthy, and much delayed, development process. Nonetheless, there are still lessons that are applicable to other rideshare missions. First, the importance of providing access to the spacecraft for as long as possible following its delivery to the launch provider and of minimizing the time between delivery and launch were two key lessons learned. Admittedly, these two factors are often out of the control of rideshare missions, but they became significant sources of concern for the LIC mission because more than one year elapsed between delivery of the spacecraft and launch. This delay led to uncertainty about the charge of the spacecraft's battery and the health of its propulsion system, but there was no ability to extract the spacecraft from its launcher or have access to the spacecraft and assess these systems.

Another lesson is the value of automating repeated processes as much as possible; this is particularly important for rideshare missions which often have to adapt to changes in the mission profile necessitated by the primary mission. The launch date of the Artemis 1 mission slipped repeatedly due to delays in launch vehicle readiness, and this necessitated the frequent redesign of the LIC baseline trajectory design. Significant time savings could have been achieved if the STK initial design to EMTG optimization part of the design process was automated earlier.

A final lesson learned that does not neatly fit into any of the categories is the fact that many aspects of the mission design and navigation process do not scale with the size of a spacecraft. If anything, they can often become more challenging as the limitations of a smaller spacecraft add new constraints on the mission design and navigation process. Because of this nonlinear relationship between spacecraft size and engineering effort, it is important for engineering teams to, as much as possible, adopt the best practices employed by larger missions when planning and executing work, even for a SmallSat mission. However, proper project management and systems engineering is costly, and a compromise must be struck between using these practices and accepting the risk of doing less. Because of the small size of the LIC team and budget, higher risks were accepted by the project. Additionally, configuration management with clearer standards and version control regarding documentation, data storage, and code sharing would have minimized some time-consuming reworks.

CONCLUSION

Some aspects of the trajectory development process and subsequent analyses outlined here are unique to LIC and its rideshare opportunity; however, many elements are applicable to any mission that seeks to conduct low-thrust trajectory design in the cislunar environment. Moreover, it is likely that opportunities for missions like LIC will occur again, not only on future Artemis missions, but on the variety of other lunar missions planned for the decade ahead. Given this trend, it is vital to disseminate lessons learned from LIC and similar missions even if the objectives of these missions were not fully realized. This document details lessons learned both in the trajectory design and early operational phases of the LIC mission including: successful design techniques, the challenges of creating a nimble design process that could quickly respond to launch date slips, and practical considerations that must be incorporated into the ConOps for a CubeSat utilizing a rideshare. With a more complete understanding of the challenges, future missions can build upon the successes and failures of LIC.

ACKNOWLEDGMENT

The authors would like to acknowledge Steve Slojowski, Noble Hatten, Khashyar Parsay, and Jacob Englander for their invaluable contributions to the Lunar IceCube mission.

REFERENCES

[1] B. K. Malphrus, K. Z. Brown, J. Garcia, C. Conner, J. Kruth, M. S. Combs, N. Fite, S. McNeil, S. Wilczweski, K. Haught, A. Zucherman, P. Clark, K. Angkasa, N. Richard, T. Hurford, D. Folta, C. Brambora, R. Macdowall, P. Mason, S. Hur-Diaz, J. Breeden, R. Nakamura, A. Martinez, and M. M. Tsay, "The Lunar IceCube EM-1 Mission: Prospecting the Moon for Water Ice," *IEEE Aerospace and Electronic Systems Magazine*, Vol. 34, No. 4, 2019, pp. 6–14, 10.1109/MAES.2019.2909384.

[2] R. L. Klima, C. M. Pieters, J. W. Boardman, R. O. Green, J. W. Head, P. J. Isaacson, J. F. Mustard, J. W. Nettles, N. E. Petro, M. I. Staid, J. M. Sunshine, L. A. Taylor, and S. Tompkins, "Lunar Ice Cube: Determining Volatile Systematics Via Lunar Orbiting Cubesat," *Journal of Geophysical Research E: Planets*, Vol. 116, No. 4, 2011, 10.1029/2010JE003719.

[3] D. C. Folta, N. Bosanac, A. Cox, and K. C. Howell, "The Lunar IceCube Mission Design: Construction of Feasible Transfer Trajectories with a Constrained Departure," *Advances in the Astronautical Sciences*, Vol. 158, 2016, pp. 1369–1387.

[4] D. C. Folta, N. Bosanac, A. Cox, and K. C. Howell, "The Lunar IceCube Mission Challenge: Attaining Science Orbit Parameters From a Constrained Approach Trajectory," *Advances in the Astronautical Sciences*, Vol. 160, 2017, pp. 3159–3178.

[5] N. Bosanac, A. D. Cox, K. C. Howell, and D. C. Folta, "Trajectory Design for a Cislunar CubeSat Leveraging Dynamical Systems Techniques: The Lunar IceCube Mission," *Acta Astronautica*, Vol. 144, 2018, pp. 283–296, 10.1016/j.actaastro.2017.12.025.

[6] R. Pritchett, K. Howell, and D. Folta, "A Trajectory Design Framework Leveraging Low-Thrust for the Lunar IceCube Mission," *5th IAA Conference on University Satellite Missions and CubeSat Workshop*, Rome, Italy, 2020, pp. 1–21.

[7] P. E. Gill, W. Murray, and M. A. Saunders, "SNOPT: An SQP Algorithm for Large-Scale Constrained Optimization," *SIAM Journal on Optimization*, Vol. 12, No. 4, 2002, pp. 979–1006, 10.1137/S1052623499350013.

[8] P. E. Gill, W. Murray, and M. a. Saunders, "User Guide for SNOPT Version 7," tech. rep., University of California, San Diego, 2008, 10.1080/10556789908805756.

[9] J. Englander, *Automated Trajectory Planning for Multiple-Flyby Interplanetary Missions*. PhD thesis, University of Illinois Urbana-Champaign, 2013.

[10] J. A. Englander and A. C. Englander, "Tuning Monotonic Basin Hopping: Improving the Efficiency of Stochastic Search as Applied to Low-Thrust Trajectory Optimization," *International Symposium on Space Flight Dynamics 2014*, Vol. 24, Laurel, MD, 2014, pp. 1–33.

[11] J. A. Englander, D. C. Folta, and S. H. Hur-Diaz, "Optimization of the Lunar Icecube Trajectory Using Stochastic Global Search and Multi-Point Shooting," *AAS/AIAA Astrodynamics Specialist Conference*, Lake Tahoe, CA, 2020, pp. 1–16.

[12] "BIT-3 RF Ion Thruster," 2023.

[13] J. S. Parker and R. L. Anderson, *Low-energy lunar trajectory design*, Vol. 12. Somerset: WILEY, 2014.

[14] R. Whitley and R. Martinez, "Options for Staging Orbits in Cis-Lunar Space," *IEEE Annual Aerospace Conference*, Big Sky, Montana, 2016, pp. 1–9, 10.1109/AERO.2016.7500635.

[15] R. Whitley, R. Martinez, G. Condon, J. Williams, and D. Lee, "Targeting Cislunar Near Rectilinear Halo Orbits for Human Space Exploration," *AAS/AIAA Astrodynamics Specialist Conference*, Stevenson, WA, 2017, pp. 1–20.

[16] Morehead State University, Busek Company, NASA Goddard Space Flight Center, JPL, and NASA IVV, "Report for Option 3: Milestone 27 Final Report," tech. rep., Morehead State University, Morehead, KY, 2023.

[17] J. Knittel, K. Hughes, J. Englander, and B. Sarli, "Automated Sensitivity Analysis of Interplanetary Trajectories for Optimal Mission Design," *International Symposium on Space Flight Dynamics*, Matsuyama, Japan, 2017, pp. 1–8.